University of Toronto

Assessing the recyclability of polyethylene terephthalate when treated with an advanced coating.

MIE498H1: Research Thesis Report

by

Kirti Saxena

Supervisor

Professor Kevin Golovin

Abstract:

This thesis investigates the recyclability of a polyester fabric made from polyethylene terephthalate (PET) when treated with an advanced hydrophobic polydimethylsiloxane (PDMS) coating applied through an iron-catalyzed reaction, designed to reduce microfiber shedding. To simulate mechanical recycling, both coated and uncoated PET samples were shredded and hot pressed into tensile dog-bone specimens at 260 °C and 270 °C. Fourier-transform infrared spectroscopy (FTIR) analysis confirmed the preservation of PET's molecular structure before and after processing, with major absorption peaks aligning with the characteristic ranges of virgin PET (1712 cm^{-1} for C=O stretching, 1238 cm^{-1} for C–O stretching, 720 cm^{-1} for CH_2 out-of-plane bending, 2920–2942 cm^{-1} for aliphatic C–H stretching, and 3330–3408 cm^{-1} for O–H stretching, potentially due to moisture or degradation). Despite the chemical stability, tensile testing revealed a decline in mechanical performance in coated samples. While uncoated PET achieved tensile strengths of 5.42 ± 0.63 MPa and Young's moduli of 0.219 ± 0.010 GPa, coated PET samples exhibited even lower tensile strengths of 1.03 ± 0.33 MPa and moduli of 0.042 ± 0.007 GPa. These results suggest that although the coating does not alter PET's chemical backbone, it may contribute to polymer chain scission or interfere with interfacial bonding during processing, leading to a possible reduction in mechanical performance. As a potential solution, the study proposes the use of reactive extrusion with chain extenders to restore strength and stiffness in coated, recycled PET materials.

Acknowledgements:

I would like to express my sincere gratitude to everyone who has supported me throughout the research and completion of this thesis. First and foremost, I extend my deepest appreciation to my supervisor, Kevin Golovin, for their invaluable guidance, insightful feedback, and allowing me access to the DREAM Laboratory. Their expertise and mentorship have been instrumental in shaping this research. I would also like to thank Weiming Li, Nathan Chang, Sudip Lahiri, Tomas Bernreiter for their assistance in experimental procedures, data analysis, and insightful discussions that contributed significantly to the development of this work. Lastly, I would like to acknowledge the University of Toronto Mechanical Engineering Department for providing the necessary resources, laboratory facilities, and financial support that made this research possible. This thesis would not have been possible without the collective efforts and support of those mentioned above.

Table of Contents:

List of Symbols:

1. Polyethylene terephthalate (PET)
2. Fourier-transform infrared (FTIR)
3. Polydimethylsiloxane (PDMS)
4. Hydrochloric Acid (HCl)
5. ATR (Attenuated Total Reflectance)
6. Isopropanol (IPA)
7. Deionized (DI)
8. APTES (3-aminopropyltriethoxysilane)
9. Dimethyldimethoxysilane (DMDMS)
10. Iron (III) p-toluenesulfonate hexahydrate ($Fe(OTs)_3$)
11. Microplastic Fibres (MPFs)

List of Figures:

List of Tables:

Chapter 1: Introduction

1.1 Introduction

Polyester produced from polyethylene terephthalate (PET) is a dominant textile material in the global market due to its cost-effectiveness, mechanical durability, lightweight nature, and versatility [1]. It can be molded into a variety of products, including single-use packaging materials, apparel, industrial components, and technical textiles [1] [2]. Despite the widespread use of PET, the increasing consumption of plastic-based products over recent decades has led to growing environmental concerns [1] [2]. In Canada, plastics from textiles contribute to approximately 7% of national plastic waste and are among leading sources of microplastic pollution in marine environments, raising significant concerns regarding long-term ecological and human health effects [3]. Figure 1 below provides a general overview of how microplastics enter the environment and the impacts they can have.

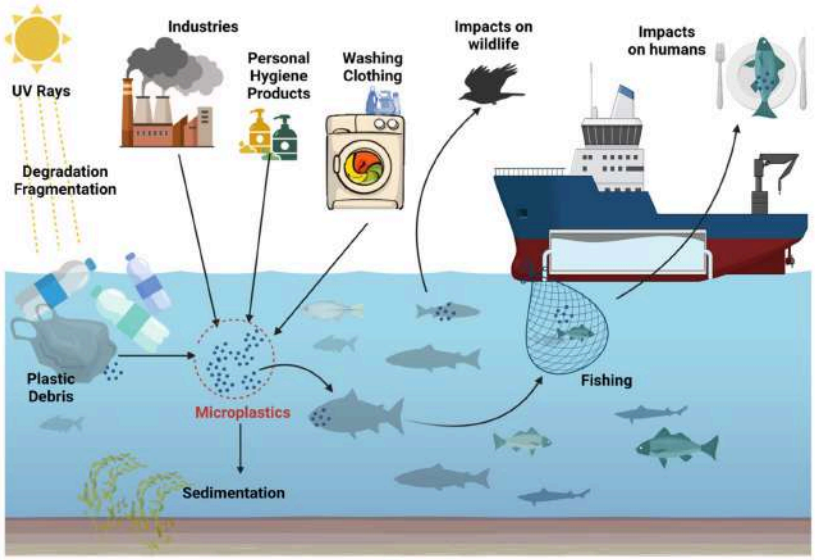

Figure 1: How microplastics affect the environment [4]

To mitigate microfibre release during laundering, the exploration of hydrophobic surface treatments that reduce fibre shedding has become a research focus within the University of Toronto's D.R.E.A.M laboratory, led by Professor Kevin Golovin. One approach involves the application of polydimethylsiloxane (PDMS) brushes, which forms a hydrophobic barrier on textile surfaces [5]. Unlike traditional solvent-based coatings, PDMS can be applied through a waterborne formulation, eliminating the need for volatile organic compounds and improving both environmental safety and manufacturing efficiency.

1.2 Justification

Understanding whether advanced coatings alter the recyclability of PET is essential, as such surface treatments may interfere with downstream processing steps. Given PET's global dominance as a widely used textile material, it is critical to assess how innovations like hydrophobic surface coatings influence its end-of-life cycle. This thesis evaluates whether polyester fabrics treated with this specific PDMS coating can still be effectively recycled and addresses a knowledge gap by experimentally simulating the recycling process for both coated and uncoated PET fabrics.

During typical workflows, PET is recycled and then reprocessed into new forms by extrusion or hot pressing. Analytical techniques are then used to assess the extent of degradation or retention of material performance. Among these techniques, Fourier-transform infrared (FTIR) spectroscopy is used to detect changes in chemical bonding or molecular structure, while tensile testing evaluates physical performance characteristics such as strength, stiffness, and ductility

[6]. When combined, these methods offer an evaluation of whether recycled PET maintains properties suitable for continued application or is compromised by the coating treatment [6].

1.3 Objectives

The primary objective of this research is to determine whether the application of an iron-catalyzed, waterborne PDMS coating impacts the recyclability of polyester (PET) fabric. This study focuses on recycling and then evaluating the performance and structural integrity of coated and uncoated PET after undergoing the simulated recycling.

To achieve this goal, the following objectives are established within the list below:

1. To prepare coated and uncoated polyester samples for testing using a consistent application method for the PDMS formulation.
2. To simulate mechanical recycling by shredding PET fabric using a blender and reforming the material through hot pressing.
3. To assess chemical structure differences between coated and uncoated recycled PET using Fourier-transform infrared (FTIR) spectroscopy.
4. To compare mechanical performance through tensile testing of both sample types, analyzing parameters such as tensile strength, elongation at break, and stiffness.
5. To evaluate whether the applied coating influences the recyclability of polyester in terms of chemical integrity and mechanical usability.

Through these objectives, this study aims to make a meaningful contribution to sustainable textile engineering by exploring how surface coating technologies affect the recyclability of synthetic fabrics.

1.4 Constraints

This study is limited by a few constraints, both in scope and methodology. They are described in the list below:

1. The research is limited to one synthetic fiber type, polyethylene terephthalate (PET), and to a single method of fabric construction, despite the many ways PET can be processed and manufactured.
2. Only one type of coating is investigated, meaning results may not be generalizable to other coating chemistries.
3. The recycling simulation is conducted through mechanical shredding of the material by the use of a 1500 W power blender, which may not capture the full complexity of industrial recycling processes.
4. The FTIR and tensile tests are performed on reprocessed samples by hot pressing only.

These constraints are acknowledged to ensure a clear understanding of the context and applicability of the research outcomes.

Chapter 2: Literature Review

2.1 Advanced Surface Coating

Advanced surface treatments can reduce microfiber shedding from PET textiles and help limit microplastic pollution. These coatings change the fiber's surface chemistry or morphology to improve wettability or reduce friction [7] [8]. Making polyester more hydrophilic through chemical alkalization or plasma treatment can increase water uptake and alter fibre interactions, reducing microfiber release by 70-90% [7] [8]. Hydrophobic nano coatings create smooth, low-friction surfaces that reduce abrasion and achieve reductions in fibre shedding during washing. By improving surface smoothness, fibre bonding, or lubricity, coatings reduce microfiber loss and microplastic release during laundering [9].

The PDMS coating used in this research (hydrophobic nano coating) was synthesized using an iron-catalyzed mechanism, which forms PDMS brushes on polyester surfaces. This method outperforms conventional hydrolysis-based approaches, such as acid-catalyzed treatments with hydrochloric acid (HCl).

2.2 Hot Pressing PET

To analyze both uncoated and coated samples of recycled PET, tensile testing was selected as one of the evaluation methods. Preparing for this test required forming the PET into standardized dog-bone specimens. To achieve this, the samples were hot pressed into the desired shape. Hot pressing PET at 260 °C (melting range is near 250-260°C) involves heating the polymer into a molten state and compressing it under high pressure, then cooling to solidify [10]. At this

temperature, PET transitions into a disordered random-coil melt, allowing polymer chains to rearrange and then recrystallize when cooled, into a semi-crystalline structure [11]. For this thesis, two rounds of uncoated and coated PET were hot pressed at 260°C and 270°C, although only the samples produced at 260°C were viable for tensile testing. The mold used to create the dog bone specimens is shown within Figure 2, and a schematic explaining the dog bone specimen type (type V was selected) is shown within Figure 3 below.

Figure 2: Mold used to hotpress dog bone specimens

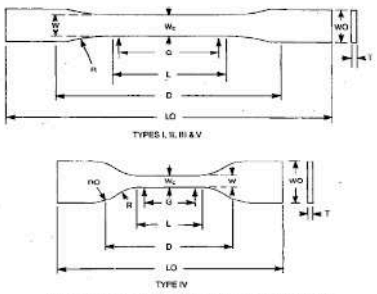

Specimen Dimensions for Thickness, *T*, mm (in.)[A]

Dimensions (see drawings)	7 (0.28) or under		Over 7 to 14 (0.28 to 0.55), incl	4 (0.16) or under		Tolerances
	Type I	Type II	Type III	Type IV[E]	Type V[C,D]	
W—Width of narrow section[C,F]	13 (0.50)	6 (0.25)	19 (0.75)	6 (0.25)	3.18 (0.125)	±0.5 (±0.02)[B,C]
L—Length of narrow section	57 (2.25)	57 (2.25)	57 (2.25)	33 (1.30)	9.53 (0.375)	±0.5 (±0.02)[C]
WO—Width overall, min[G]	19 (0.75)	19 (0.75)	29 (1.13)	19 (0.75)	...	+ 6.4 (+ 0.25)
WO—Width overall, min[G]	...	...	...	...	9.53 (0.375)	+ 3.18 (+ 0.125)
LO—Length overall, min[H]	165 (6.5)	183 (7.2)	246 (9.7)	115 (4.5)	63.5 (2.5)	no max (no max)
G—Gage length[I]	50 (2.00)	50 (2.00)	50 (2.00)	...	7.62 (0.300)	±0.25 (±0.010)[C]
G—Gage length[I]	...	...	...	25 (1.00)	...	±0.13 (±0.005)
D—Distance between grips	115 (4.5)	135 (5.3)	115 (4.5)	65 (2.5)[J]	25.4 (1.0)	±5 (±0.2)
R—Radius of fillet	76 (3.00)	76 (3.00)	76 (3.00)	14 (0.56)	12.7 (0.5)	±1 (±0.04)[C]
RO—Outer radius (Type IV)	...	...	...	25 (1.00)	...	±1 (±0.04)

Figure 3: Dog bone specimen types and tolerances [12]

2.3 Methods of Analysis

To understand the potential and limitations of PET recycling, it is important to highlight the various methods used to process and repurpose PET materials. As shown in Figure 4, PET can be recycled through three main approaches: Primary (re-extrusion), Secondary (mechanical), and Tertiary (chemical) recycling [13]. Each method differs in complexity, cost, and the quality of the output [13]. Primary and secondary methods preserve the polymer structure, whereas tertiary recycling breaks PET down into fundamental chemical components, like monomers and dimers [13]. The selection of a recycling method influences the resulting material properties and end-use applications, making it one of the key considerations when assessing the overall sustainability and effectiveness of PET reuse.

For the purpose of this thesis, mechanical recycling was selected due to it being a straightforward process and the ability to retain the polymer structure. This aligns with the study's goal of comparing the performance of uncoated and coated PET in their recycled polymer form. In a typical recycling workflow, PET is shredded and reprocessed (extrusion or hot-pressing) into new samples, and analytical techniques are applied to assess its recyclability. Fourier-transform infrared spectroscopy and tensile testing are two complementary methods widely used for this purpose [15] [16]. FTIR reveals any chemical structural changes in PET after recycling, while tensile tests evaluate the material's mechanical integrity compared to virgin PET. Together, these methods help determine if recycled PET retains suitable properties for continued use [15] [16].

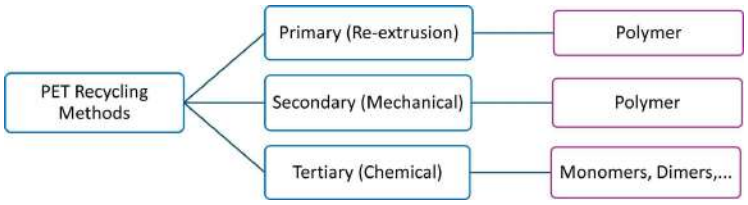

Figure 4: PET recycling methods [13]

2.3.1 Fourier-Transform Infrared Spectroscopy

Fourier Transform Infrared Spectroscopy is a modern infrared-based analytical technique valued for its high precision, speed, sensitivity, and non-destructive testing [16]. It operates on the principle that molecules absorb specific infrared frequencies corresponding to their atomic vibrations, producing unique spectral patterns that allow for molecular identification [16]. An interferometer encodes the infrared signal before it interacts with the sample [16]. As the beam passes through or reflects off the sample, specific wavelengths are absorbed [16]. The remaining signal is detected and processed via Fourier transformation to generate the infrared spectrum. [16]. Figure 5 shows the ATR (attenuated total reflectance) attachment which enables direct analysis of samples by using total internal reflection to generate an evanescent wave that interacts with the sample [14].

PET's FTIR spectrum has characteristic peaks for its ester linkages and aromatic rings [17]. After mechanical recycling, these signature peaks generally remain, confirming that the base polymer structure is still PET [18] [19]. Therefore, FTIR serves as a crucial tool to ensure the recycled PET's chemical purity and to monitor any degradation chemistry (like oxidation, chain scission, or crosslinking) that might not be visible otherwise [18] [19]. Shown in the Figure 6

below is the FTIR spectrum of PET and Table 1 explains what chemical composition the peaks describe.

Figure 5 : ATR attachment for FTIR spectroscopy testing recycled PET

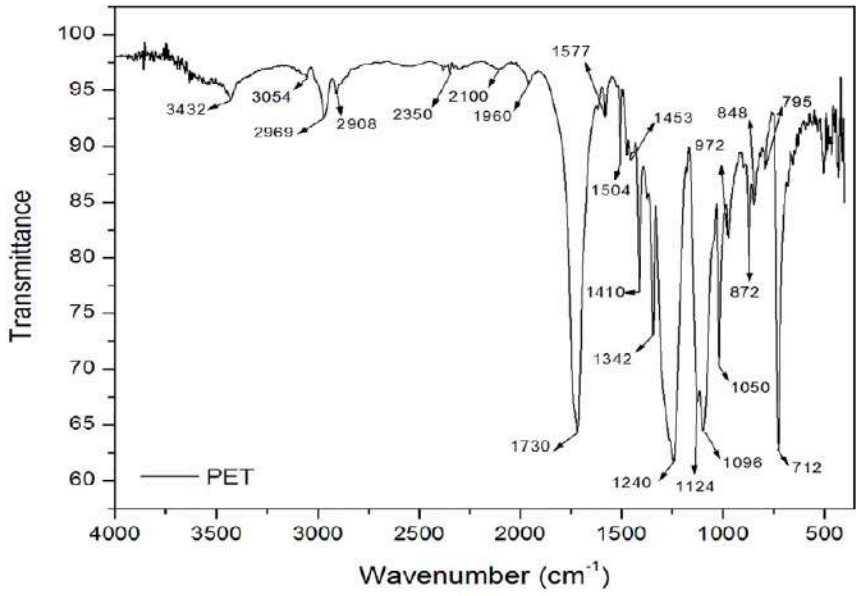

Figure 6: The general FTIR spectrum of PET [17]

Table 1: Bands with vibrational modes from the FTIR spectrum of PET [17]

Absorption Bands	Bands
3432	OH group (hydroxyl)[19,20]
3054	Symmetrical stretch of CH[20]
2969 and 2908	C-H, Symmetrical stretching[20]
1730	Stretching of C=O of carboxylic acid group[19]
1577 or 1504	Vibrations aromatic skeleton with stretching C=C[19]
1453, 1410 and 1342	Stretching of the C-O group deformation of the O-H group[19,20] and bending and wagging vibrational modes of the ethylene glycol segment[21]
1240 or 1124	Terephthalate Group (OOCC6H4-COO)[19]
1096 or 1050	Methylene group[21] and vibrations of the ester C-O bond[20]
972, 872, 848	Aromatic rings 1,2,4,5; Tetra replaced[19,20]
1960 and 795	Vibrations of adjacent two aromatic H in p-substituted compounds[19,20] and aromatic bands[21]
712	Interaction of polar ester groups and benzene rings[19]

2.3.2 Tensile Dog Bone Testing

Tensile testing is a method for assessing the mechanical performance of recycled PET. This process involves using a PET sample that is shaped into a dog-bone as shown in Figure 7. Uniaxial tension is applied to the specimen until failure, which is done by clamping both sides of the dogbone and pulling apart until it breaks as shown in Figure 8. Key properties measured include Young's modulus (stiffness), tensile strength and load versus displacement [20]. These metrics provide direct insight into the material's structural integrity. When PET is mechanically recycled, it can induce polymer chain scission, from thermal or hydrolytic degradation, reducing the molecular weight of PET [20]. Shorter chains typically lead to lower tensile strength and especially reduced elongation meaning more brittleness, since the material's ability to carry load and deform without breaking is impaired [20].

Figure 7: PET sample molded into dog bone shape

Figure 8: Clamps pulling apart dogbone specimen

Chapter 3: Experimental Procedure

3.1 Adding the PDMS brush coating to PET

The coating process was carried out by PhD student Weiming Li, who provided the following detailed description. Prior to coating the polyester textile, samples were cleaned by three 30 minute sonication cycles, alternating between isopropanol (IPA) and deionized (DI) water to remove residual contaminants, and then dried in an oven at 65 °C for 4 hours [21]. Polyester and silicon wafer samples were treated with oxygen plasma for 10 minutes at 45 W using a Harrick Plasma Cleaner to activate the surfaces [21]. To facilitate bonding of PDMS brushes to the polyester surface, a polyester specific APTES primer was prepared by dissolving 1% v/v APTES in toluene and applying it with a dip-coating [21]. After a 24-hour immersion, the samples were rinsed thoroughly with toluene, hydrolyzed in an acidic water solution (pH 4.5–5.0) for 6 hours, rinsed with DI water, and dried with compressed air at room temperature [21]. Prior to polymer brush deposition, the samples were again exposed to oxygen plasma for 2 minutes to convert remaining ethoxy groups to silanol groups [21]. PDMS brushes were grown by vapor-phase deposition of 1, 3-dichlorotetramethyldisiloxane (DCTMDS) for 1 hour at room temperature in a closed container. Following deposition, samples were rinsed with IPA and toluene and dried with compressed air [21].

3.2 Mechanically Recycling Material

The PET fabric was made up of 100% polyester, onesided fleece and prefinished fabrics with a weight of approximately 180 g m−2 which were received from Arc’teryx and shredded using a CRANDDI Commercial 1500 W power blender [22]. As a preliminary trial, uncoated PET fabric

was tested first. It was observed that running the blender for more than six seconds at a time caused the polymer to overheat and partially burn. Based on this observation, the coated PET was shredded using a pulsed approach to prevent thermal damage. The PET fabric swatches shown in Figure 9 were first cut into smaller pieces with scissors and then shredded into finer particles using the blender.

Figure 9: Process of mechanically recycling PET

3.3 Hot Pressing Uncoated and Coated PET Samples

The shredded fibers, as shown in Figure 9, were placed into the center of the mold depicted in Figure 2 and hot pressed into dogbones. Two temperatures were tested during this process: 270°C and 260°C. The resulting hot pressed samples made from the uncoated PET, as seen in Figure 10, appeared black at first glance. However, upon closer inspection and with a focus on the excess material around the dog-bone structure, revealed an orange hue. This indicated that the original color of the material remained unchanged through hot pressing and the perceived

blackness was due to the increased thickness and layering of the material, which affected the way it reflected light.

The dog-bone specimens made from the coated PET hot pressed at 260°C appeared multicolored with one end resembling the black uncoated samples, while the other displayed a fibrous yellow texture. Compared to the uncoated counterparts, these samples were noticeably more brittle to the touch, though they could still be successfully removed from the mold. In contrast, specimens made from the coated PET and processed at 270°C were uniformly black but exhibited extreme brittleness, breaking apart and failing to release from the mold upon cooling. Both samples are shown in Figure 11.

Figure 10: Hot pressed dog bone specimens of uncoated PET at 270°C and 260°C

Figure 11: Hot pressed dog bone specimens made from coated PET at 270°C and 260°C

Chapter 4: Results and Discussion

4.1 Results

FTIR analysis was conducted on both coated and uncoated PET samples under four conditions: unrecycled, mechanically shredded, and hot pressed at either 260 °C or 270 °C. An exception for the coated recycled sample hot pressed at 260 °C was made as one side of the dog bone sample appeared black and the other side exhibited a yellow fibrous texture, as shown in Figure 11. Both sides were analyzed to determine if any chemical changes had occurred. Tensile testing was performed on the hot pressed samples processed at 260 °C, as the coated samples hot pressed at 270 °C could not be removed intact from the mold. For each FTIR spectrum, major peaks were examined and compared to the reference PET spectrum provided in Figure 6.

4.1.1 FTIR spectrum of Uncoated PET

The data indicates that the PET structure remains intact, as most peak values fall within the wavenumber ranges specified in Table 1. Overall, the spectra graphs shown in Figure 12 closely resembled the original PET spectrum described in Figure 6. All individual graphs and data points can be referenced to within Appendices A.

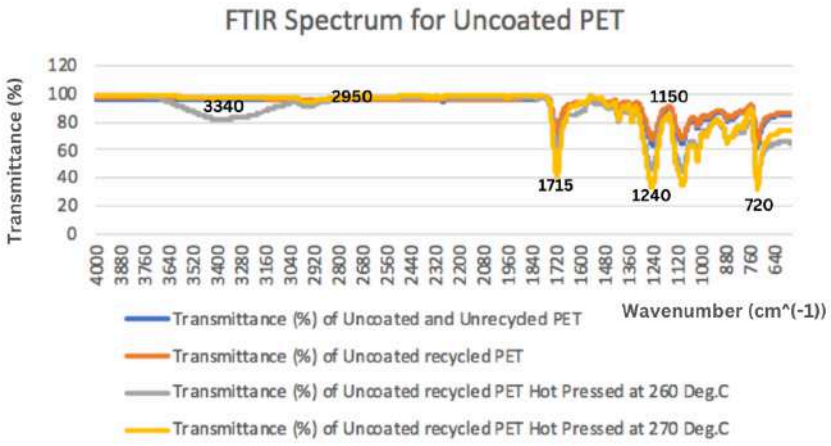

Figure 12: Spectra graphs of uncoated PET in different cases

4.1.2 FTIR Spectrum of Coated PET

The same peaks were used to compare the measured spectra with the reference PET spectrum shown in Figure 6. The data indicates that the PET structure remains intact, as most peak values fall within the ranges of values in Table 1, as shown in Figure 13. The graphs for each case as well as a table outlining specific data points can be found in Appendix B.

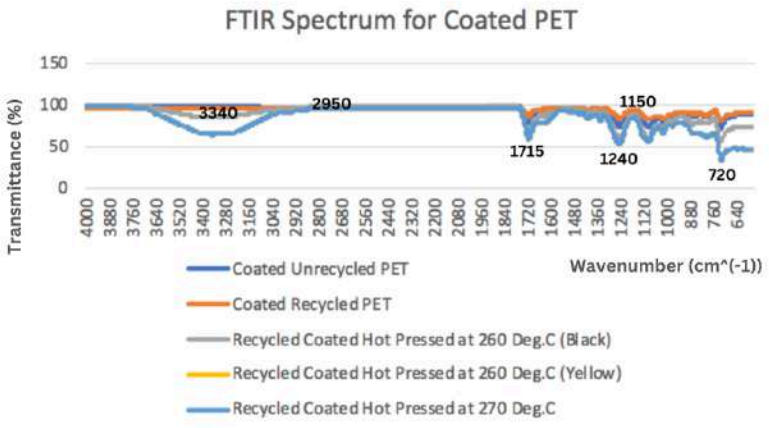

Figure 13: Spectra graphs of coated PET in different cases

4.2 Tensile Testing

Tensile testing was conducted only on the uncoated and coated recycled PET samples that were hot pressed at 260°C. While the uncoated specimens processed at 270°C were structurally sound and viable for testing, the coated samples processed under the same conditions were extremely brittle and fractured at the neck during removal from the mold shown in Figure 2.

For both uncoated and coated recycled samples, the tensile test results were expected to deviate due to sample curvature and incomplete flatness from the pressing process. Given these limitations, it was more appropriate to use the viable uncoated and coated samples for a comparative analysis, rather than relying solely on the absolute tensile test values. Although the coated 260°C samples were more brittle than their uncoated counterparts, they were sufficiently intact to be successfully removed from the mold and tested, but even then a few of them slipped during testing as shown in Figure 14. By the data gathered from testing as shown in Table 2, there were a few consistent calculations made for each tensile test run. A snippet of the output data is shown in Figure 15 and the following calculations for cross sectional area and tensile stress and were completed for each dogbone tested:

$$Cross\ Sectional\ Area\ =\ Width\ *\ Thickness$$

$$=\ 15\,mm\ *\ 5\,mm\ =\ 75\,mm^2\ =\ 7.5\ *\ 10^{-5}m^2$$

$$Tensile\ Strength\ =\ Force/Area\ =\ 424.16\,N/7.5\ *\ 10^{-5}mm\ =\ 5.66\,MPa$$

The Young's modulus was then calculated by taking the linear regression of load versus displacement curves which can be found in Appendix C.

Table 2: Given values from tensile testing data collected for uncoated PET sample #1

Width	15 mm
Thickness	5 mm
Gauge Length	25 mm
Maximum Load	0.42416 kN
Maximum Extension	77.03 mm

Figure 14: Example of a testing sample that slipped and broke at one end

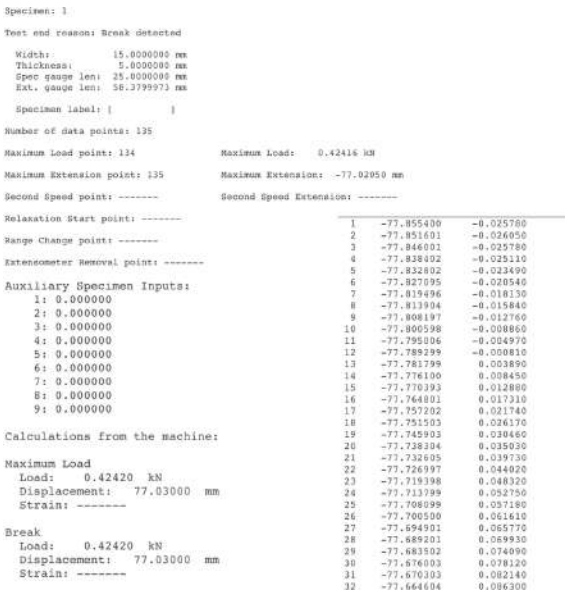

```
Specimen: 1

Test end reason: Break detected

  Width:           15.0000000 mm
  Thickness:        5.0000000 mm
  Spec gauge len:  25.0000000 mm
  Ext. gauge len:  58.3799973 mm

  Specimen label: |          |

Number of data points: 135

Maximum Load point: 134              Maximum Load:    0.42416 kN

Maximum Extension point: 135         Maximum Extension:  -77.02950 mm

Second Speed point: -------          Second Speed Extension: -------

Relaxation Start point: -------

Range Change point: -------

Extensometer Removal point: -------

Auxiliary Specimen Inputs:
    1: 0.000000
    2: 0.000000
    3: 0.000000
    4: 0.000000
    5: 0.000000
    6: 0.000000
    7: 0.000000
    8: 0.000000
    9: 0.000000

Calculations from the machine:

Maximum Load
  Load:     0.42420  kN
  Displacement:    77.03000  mm
  Strain: -------

Break
  Load:     0.42420  kN
  Displacement:    77.03000  mm
  Strain: -------
```

1	-77.855400	-0.025780
2	-77.851601	-0.026050
3	-77.846001	-0.025780
4	-77.838402	-0.025110
5	-77.832802	-0.023490
6	-77.827095	-0.020540
7	-77.819496	-0.018130
8	-77.813904	-0.015840
9	-77.808197	-0.012760
10	-77.800598	-0.008860
11	-77.795006	-0.004970
12	-77.789299	-0.000810
13	-77.781799	0.003890
14	-77.776100	0.008450
15	-77.770393	0.012880
16	-77.764801	0.017310
17	-77.757202	0.021740
18	-77.751503	0.026170
19	-77.745903	0.030460
20	-77.738304	0.035030
21	-77.732605	0.039730
22	-77.726997	0.044020
23	-77.719398	0.048320
24	-77.713799	0.052750
25	-77.708099	0.057180
26	-77.700500	0.061610
27	-77.694901	0.065770
28	-77.689201	0.069930
29	-77.683502	0.074090
30	-77.676003	0.078120
31	-77.670303	0.082140
32	-77.664604	0.086300

Figure 15: Snippet of the output data from tensile testing

4.2.1 Uncoated PET Tensile Testing

Five samples of uncoated recycled PET hot pressed at 260°C were tensile tested as shown in Figure 16. All specimens underwent tensile testing, and the results are presented in Table 3. The tensile strength value for PET 5 was excluded from the final calculations, as the result was substantially lower than other samples.

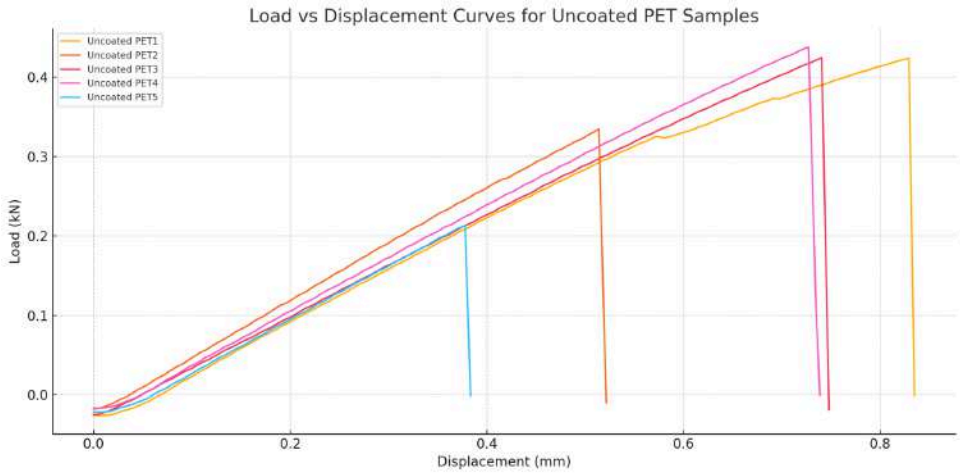

Figure 16: Load versus displacement curve for uncoated PET

Table 3 : Uncoated recycled PET samples tensile testing data

Sample	**Tensile Strength (MPa)**	**Young's Modulus (GPa)**
Uncoated PET 1	5.66	0.210
Uncoated PET 2	4.48	0.235
Uncoated PET 3	5.67	0.211
Uncoated PET 4	5.88	0.214
Uncoated PET 5	2.84	0.227

4.2.2 Coated PET Tensile Testing

Five samples of coated recycled PET hot pressed at 260°C were tensile tested as shown in Figure 17. Unfortunately, samples 4 and 5 experienced slippage at the clamp during tensile testing, which compromised the accuracy of the force displacement data. As a result, the tensile strength values for both samples and the Young's modulus for PET 5 were excluded from the final calculations. The corresponding data calculated is below in Table 4.

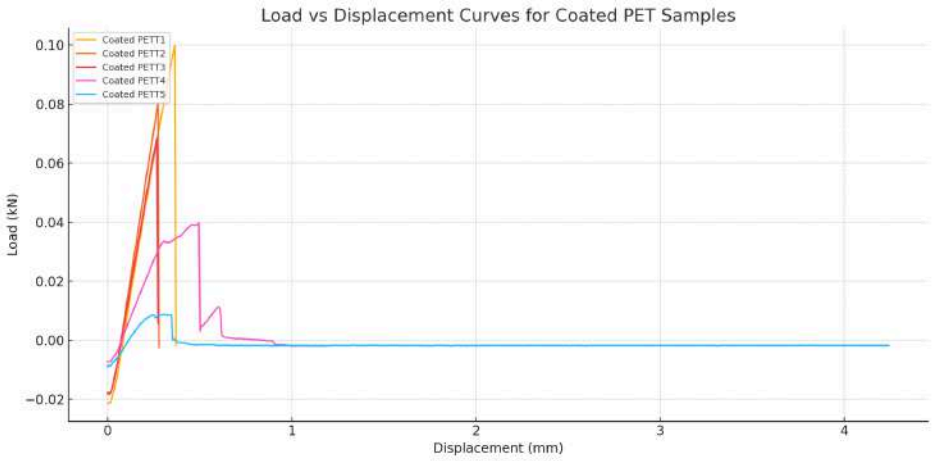

Figure 17: Load versus displacement curve for coated PET

Table 4: Coated recycled PET samples tensile testing data

Sample	**Tensile Strength (MPa)**	**Young's Modulus (GPa)**
Coated PET 1	1.33	0.045
Coated PET 2	1.07	0.032
Coated PET 3	0.68	0.045
Coated PET 4	0.71	0.047
Coated PET 5	0.12	0.015

4.3 Discussion

The coated PET samples retained the molecular structure of polyethylene terephthalate, which is confirmed by FTIR spectra analysis as shown in Figures 12 and 13. However, the samples exhibited a decline in mechanical performance. Both tensile strength and Young's modulus dropped significantly compared to typical values observed in recycled PET, which generally retains a tensile strength of 48–49 MPa and a modulus of 2.1–2.2 GPa [23] [24] [25]. Both the uncoated and coated samples in this study fell below typical tensile strength benchmarks. In the case of the uncoated samples, this deviation may be due to the curvature introduced during the pressing process, as previously hypothesized. For the coated samples, the results suggest that while the coating process preserved the polymer's chemical integrity, it adversely affected the material's structural stiffness and load-bearing capacity. A high level overview of the comparison is described within Table 5 below. Figure 18 presents the stress-strain curves for the tested samples. The coated samples exhibit a lower and more inconsistent slope, indicating brittle behavior. In contrast, the uncoated samples display a well-defined, steeper slope, characteristic of more ductile materials. Individual graphs for coated and uncoated samples can be found in Appendix D.

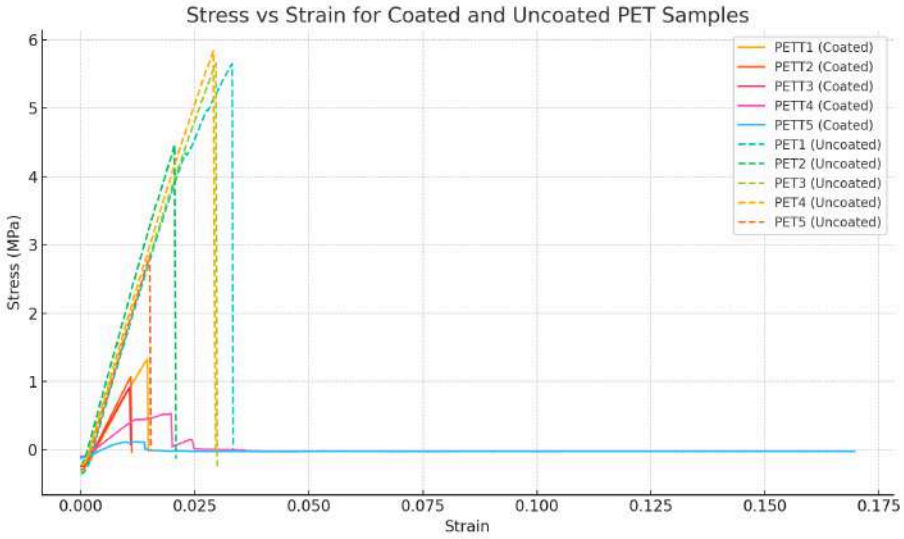

Figure 18: Stress versus strain curve for coated and uncoated PET samples

Table 5: Describing the data from tensile testing calculations and comparing to reference data [23] [24] [25]

Property	**Reference Value for Recycled PET**	**Observation in Coated Samples**	**Observation in Uncoated Samples**
Young's Modulus	2.1 GPa	0.042 ± 0.007 GPa (omitted PET 4, PET 5)	0.219 ± 0.010 GPa
Tensile Strength	48 MPa	1.03 ± 0.33 MPa (omitted PET 5)	5.42 ± 0.63 MPa (omitted PET 5)

4.4 Analysis

The coated PET samples, particularly those hot-pressed at 270°C, exhibited high brittleness during mold removal, suggesting possible thermal degradation of the coating or interfacial layers [26]. This degradation may have compromised structural cohesion, caused chain scissons and

significantly reduced the material's mechanical viscoelastic properties [26]. Surface roughness and inconsistencies introduced by the coating were also observed, contributing to sample slippage during tensile testing, which was a factor that may have further underestimated the Young's modulus and strength. The coating material may be incompatible with high temperature processing, which could have introduced cracks or internal weak points making the material more susceptible to mechanical failure despite the molecular structure of PET remaining intact, as confirmed by FTIR analysis.

4.5 Obstacles

Several obstacles emerged that challenged both the experimental process and the overall direction of the research. One of the primary difficulties involved achieving consistent mechanical recycling of PET using non-industrial equipment. The use of a high-powered blender introduced variability in fiber size and heat generation. Another challenge arose during the hot pressing phase, where temperature and pressure inconsistencies, particularly at higher temperatures like 270°C, resulted in sample brittleness and incomplete mold filling. This caused samples to break when taken out of the mold. Surface roughness and non-uniform thickness in all samples led to slippage during tensile testing, making it difficult to capture accurate mechanical performance metrics. Despite these setbacks, each obstacle provided an opportunity to adapt methods, refine protocols, and gain deeper insight into the relationship between mechanical processing, surface coatings, and PET performance.

Chapter 5: Conclusion

This research evaluated the mechanical recyclability of PET treated with an iron-catalyzed PDMS coating, with a focus on structural and chemical integrity post-recycling. FTIR spectroscopy confirmed that the coating did not alter PET's molecular structure throughout the recycling process. However, tensile testing revealed a significant reduction in mechanical performance for coated samples, particularly in tensile strength and stiffness.

The test results indicate that although the advanced coating maintained chemical purity, it compromised the material's mechanical robustness. The decline in mechanical performance may be due to a reduction in molecular weight, indicating shorter PET chains in the final product [26]. Although the exact stage of the process responsible for this change remains unclear. These results point to a possible trade-off between functional surface treatments and mechanical reusability, and highlights the importance of future research focused on identifying where in the process chain scission occurs, as improving chain extension during recycling could help recover mechanical performance [26] [27]. Chain extension is generally performed through reactive extrusion, which chemically links shorter polymer chains into longer ones [26] [27]. Incorporating chain extension in future studies may offer a pathway to recovering mechanical performance in coated PET while maintaining sustainable recyclability.

Chapter 6: Summary

This thesis evaluates the compatibility of an advanced hydrophobic polydimethylsiloxane (PDMS) coating with the mechanical recycling of polyethylene terephthalate (PET). The coating, applied with an iron-catalyzed reaction, is designed to reduce microfiber shedding during laundering. To assess its impact on the mechanical performance of PET fabrics, both coated and uncoated samples were hot pressed into tensile dog-bone specimens at 260 °C and 270 °C. FTIR analysis conducted on samples before and after recycling and hot pressing confirmed the preservation of PET's chemical structure. Major absorption peaks that were consistent with virgin PET include: 1712 cm^{-1} for C=O stretching, 1238 cm^{-1} for C–O stretching, 720 cm^{-1} for CH_2 out-of-plane bending, 2920–2942 cm^{-1} for aliphatic C–H stretching, and 3330–3408 cm^{-1} for O–H stretching, possibly associated with moisture or degradation [17]. Despite the chemical stability, mechanical testing revealed that coated samples experienced a significant reduction in strength and stiffness, indicating compromised mechanical performance.

Uncoated PET exhibited tensile strengths of 5.42 ± 0.63 MPa and Young's moduli ranging from 0.219 ± 0.010 GPa . In contrast, coated PET samples achieved tensile strengths of 1.03 ± 0.33 MPa, with corresponding moduli ranging from 0.042 ± 0.007 GPa. These values fall short of the typical benchmarks for both virgin and recycled PET, which for virgin should be a tensile strength around 50-60 MPa and moduli within 2-3 GPa [23] [24] [25]. Recycled PET should be tensile strengths around 48–49 MPa and moduli in the range of 2.1–2.2 GPa [23] [24] [25]. The poor performance of the uncoated samples is likely due to physical inconsistencies introduced during processing, such as curvature and uneven thickness caused by hot pressing. For the coated samples, although FTIR results confirmed that chemical integrity was retained, the substantial

loss in mechanical strength suggests the presence of chain scission, leading to shorter PET chains [26]. This indicates that the coating or thermal processing may have affected polymer structure, further compromising mechanical performance.

Throughout experimentation, several challenges were faced, including fiber melting during recycling, dogbone specimens breaking due to brittleness, and testing slippage which contributed to error within experimentation. Despite maintaining chemical integrity, the coated PET reduced mechanical performance, which suggests degradation and thermal incompatibility of the coating [26] [27]. As a next step, reactive extrusion for chain extension is proposed to improve mechanical properties for future recycling workflows [26] [27].

References:

[1] Y.-H. V. Soong, M. J. Sobkowicz, and D. Xie, “Recent Advances in Biological Recycling of Polyethylene Terephthalate (PET) Plastic Wastes - PMC,” *Bioengineering*, vol. 9, no. 3, Feb. 2022, doi: 10.3390/bioengineering9030098.

[2] J. Boucher and D. Friot, *Primary microplastics in the oceans: A global evaluation of sources*. IUCN International Union for Conservation of Nature, 2017 [Online]. Available: https://portals.iucn.org/library/sites/library/files/documents/2017-002-En.pdf. [Accessed: 31-Mar-2025]

[3] Environment and Climate Change Canada, “Science assessment of plastic pollution,” *Canada.ca*, Oct-2020. [Online]. Available: https://www.canada.ca/en/environment-climate-change/services/evaluating-existing-substances/science-assessment-plastic-pollution.html. [Accessed: 31-Mar-2025]

[4] K. Ziani *et al.*, “Microplastics: A Real Global Threat for Environment and Food Safety: A State of the Art Review,” *Nutrients*, vol. 15, no. 3, Jan. 2023, doi: 10.3390/nu15030617.

[5] X. Zhao *et al.*, “Crosslinking inert liquidlike polydimethylsiloxane brushes using bis-diazirine chemical insertion for enhanced mechanical durability,” *Chemical Engineering Journal*, vol. 442, p. 136017, Aug. 2022, doi: 10.1016/j.cej.2022.136017.

[6] A. Lund, “Material properties of recycled PET in beverage containers,” Dissertation, 2021.

[7] P.-F. Sun, C. Rong, L. Meng, L. Wu, and H. Zhu, “Functional polymer brushes for anti-microplastic pollution,” *Eco-Environment & Health*, vol. 2, no. 3, pp. 92–94, Sep. 2023, doi: 10.1016/j.eehl.2023.06.002.

[8] A. Jabbar, M. Bryant, J. Armitage, and M. Tausif, “Oxygen plasma treatment to mitigate the shedding of fragmented fibres (microplastics) from polyester textiles,” *Cleaner Engineering and Technology*, vol. 23, p. 100851, Dec. 2024, doi: 10.1016/j.clet.2024.100851.

[9] A. P. Periyasamy, “Environmentally Friendly Approach to the Reduction of Microplastics during Domestic Washing: Prospects for Machine Vision in Microplastics Reduction,” *toxics*, 2023.

[10] ScienceDirect, “Hot Pressing - an overview,” *ScienceDirect Topics*, 2020. [Online]. Available: https://www.sciencedirect.com/topics/materials-science/hot-pressing#:~:text=Explore%20book-,Hot%20pressing%20(HP),density%20in%20a%20reasonable%20time. [Accessed: 01-Apr-2025]

[11] T. B. Thomsen, K. Almdal, and A. S. Meyer, “Significance of poly(ethylene terephthalate) (PET) substrate crystallinity on enzymatic degradation,” *New Biotechnology*, vol. 78, pp. 162–172, Dec. 2023, doi: 10.1016/j.nbt.2023.11.001.

[12] E. Liberato, “Edi Liberato blog,” *Liberato*, 2020. [Online]. Available: https://eddieliberato.github.io/blog/2020-05-14-dogbones/. [Accessed: 01-Apr-2025]

[13] M. Babaei, M. Jalilian, and K. Shahbaz, “Chemical recycling of Polyethylene terephthalate: A mini-review,” *Journal of Environmental Chemical Engineering*, vol. 12, no. 3, Jun. 2024, doi: 10.1016/j.jece.2024.112507.

[14] U. Riaz and S. M. Ashraf, “Characterization of Polymer Blends with FTIR Spectroscopy,” *unknown*, 31-Oct-2014. [Online]. Available: https://www.researchgate.net/publication/278314328_Characterization_of_Polymer_Blends_with_FTIR_Spectroscopy. [Accessed: 06-Apr-2025]

[15] D. R. Jenket, A. E. Engelbrecht-Wiggans, A. L. Forster, and M. Al-Sheikhly, “A new method for tensile testing UHMMPE single fibers at high temperatures and strain-rates,” National Institute of Standards and Technology, Gaithersburg, MD, Aug. 2019 [Online]. Available: https://nvlpubs.nist.gov/nistpubs/ir/2019/NIST.IR.8265.pdf?utm_source=chatgpt.com. [Accessed: 06-Apr-2025]

[16] Aviation Fuels, “Fourier Transform Infrared Spectrometer - an overview,” *ScienceDirect Topics*, 2021. [Online]. Available: https://www.sciencedirect.com/topics/engineering/fourier-transform-infrared-spectrometer. [Accessed: 31-Mar-2025]

[17] A. P. dos S. Pereira, M. H. P. da Silva, É. P. L. Jr, and F. Tommasini, “Processing and Characterization of PET Composites Reinforced With Geopolymer Concrete Waste,” *SciELO*, 09-Oct-2017. [Online]. Available: https://www.researchgate.net/publication/320288961_Processing_and_Characterization_of_PET_Composites_Reinforced_With_Geopolymer_Concrete_Waste. [Accessed: 02-Apr-2025]

[18] T. Muringayil Joseph *et al.*, “Polyethylene terephthalate (PET) recycling: A review,” *Case Studies in Chemical and Environmental Engineering*, vol. 9, p. 100673, Jun. 2024, doi: 10.1016/j.cscee.2024.100673. https://www.researchgate.net/figure/FT-IR-spectrum-of-the-PET-sample_fig1_320288961. [Accessed: 01-Apr-2025]

[19] B. Bhattarai, Y. Kusano, T. L. Cederberg, L. K. Jensen, K. Granby, and G. A. Pedersen, “Chemical characterization of virgin and recycled polyethylene terephthalate films used for food contact applications,” *European Food Research and Technology*, vol. 250, no. 2, pp. 533–545, Nov. 2023, doi: 10.1007/s00217-023-04400-z.

[20] Del Mar Castro Lopez, M. (2014). Assessing changes on poly(ethylene terephthalate) properties after recycling: Mechanical recycling in laboratory versus postconsumer recycled material. *Materials Chemistry and Physics*, *147*(3), 884–894. https://doi.org/10.1016/j.matchemphys.2014.06.034

[21] S. K. Lahiri, Z. A. Dijvejin, and K. Golovin, “Polydimethylsiloxane-coated textiles with minimized microplastic pollution,” *Nature Sustainability*, vol. 6, no. 5, pp. 559–567, Jan. 2023, doi: 10.1038/s41893-022-01059-4.

[22] S. K. Lahiri *et al.*, “Liquidlike, Low‐Friction Polymer Brushes for Microfibre Release Prevention from Textiles,” *Small*, vol. 20, no. 33, 2024, doi: 10.1002/smll.202400580.

[23] E. Kijeńska-Gawrońska, K. Wiercińska, and M. Bil, “The Dependence of the Properties of Recycled PET Electrospun Mats on the Origin of the Material Used for Their Fabrication - PMC,” *Polymers*, vol. 14, no. 14, Jul. 2022, doi: 10.3390/polym14142881.

[24] A. Alvarez, Q. Ma, and J. Mckenzie, “Tensile Testing for Determination of Mechanical Properties of Recycled PET-G Plastics,” *unknown*, 14-Nov-2024. [Online]. Available: https://www.researchgate.net/publication/385841364_Tensile_Testing_for_Determination_of_Mechanical_Properties_of_Recycled_PET-G_Plastics. [Accessed: 07-Apr-2025]

[25] M. Bembenek, Ł. Kowalski, and A. Kosoń-Schab, “Research on the Influence of Processing Parameters on the Specific Tensile Strength of FDM Additive Manufactured PET-G and PLA Materials,” *Polymers*, vol. 14, no. 12, Jun. 2022, doi: 10.3390/polym14122446.

[26] I. Cusano, L. Campagnolo, M. Aurilia, S. Costanzo, and N. Grizzuti, “Rheology of Recycled PET - PMC,” *Materials*, vol. 16, no. 9, 2023, doi: 10.3390/ma16093358.

[27] Z. O. G. Schyns and M. P. Shaver, “Mechanical Recycling of Packaging Plastics: A Review,” *Macromolecular Rapid Communications*, vol. 42, no. 3, 2020, doi: 10.1002/marc.202000415.

Appendices:

Appendix A: FTIR Graphs of Uncoated PET and Data Points of Major Peaks

This appendix shows the FTIR spectra of coated PET within Figures 19 to 22 and highlights major peak data points within Table 6.

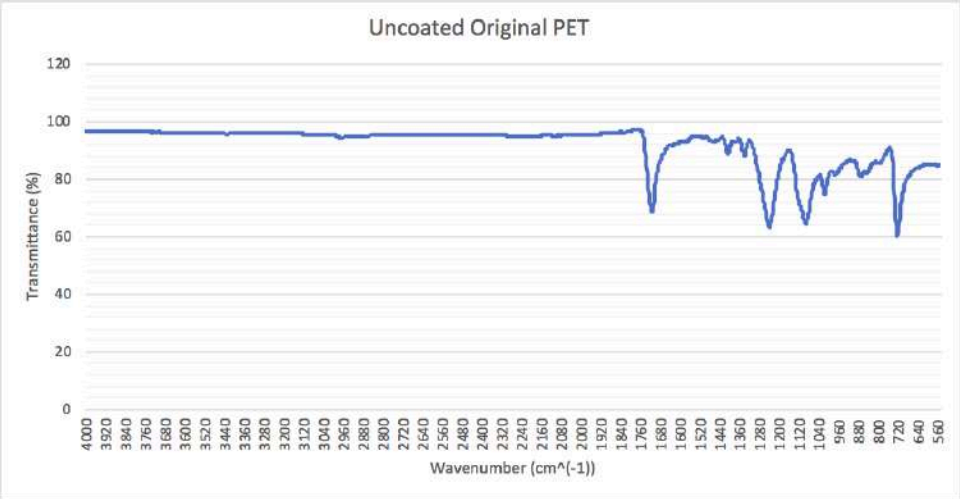

Figure 19: FTIR Spectra of original PET

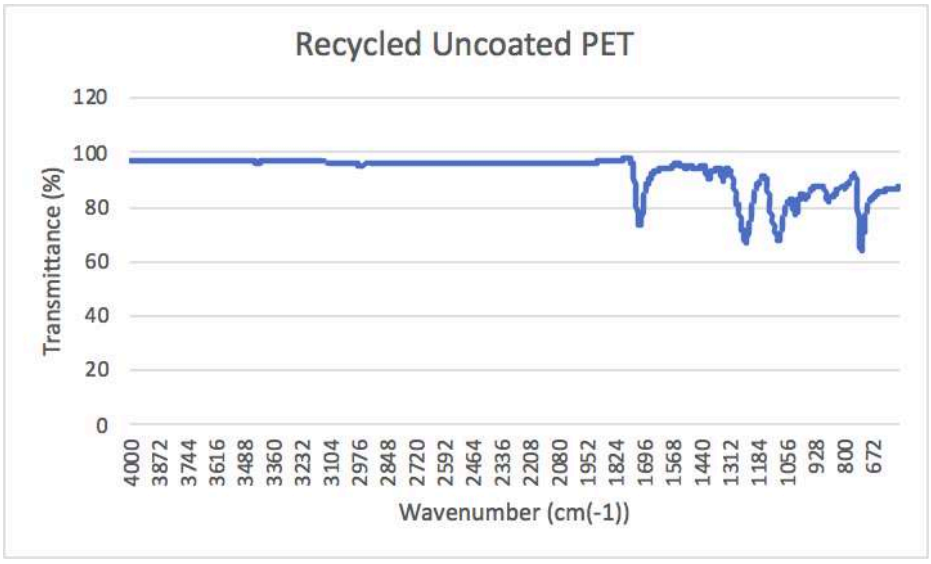

Figure 20 : FTIR Spectra of original PET

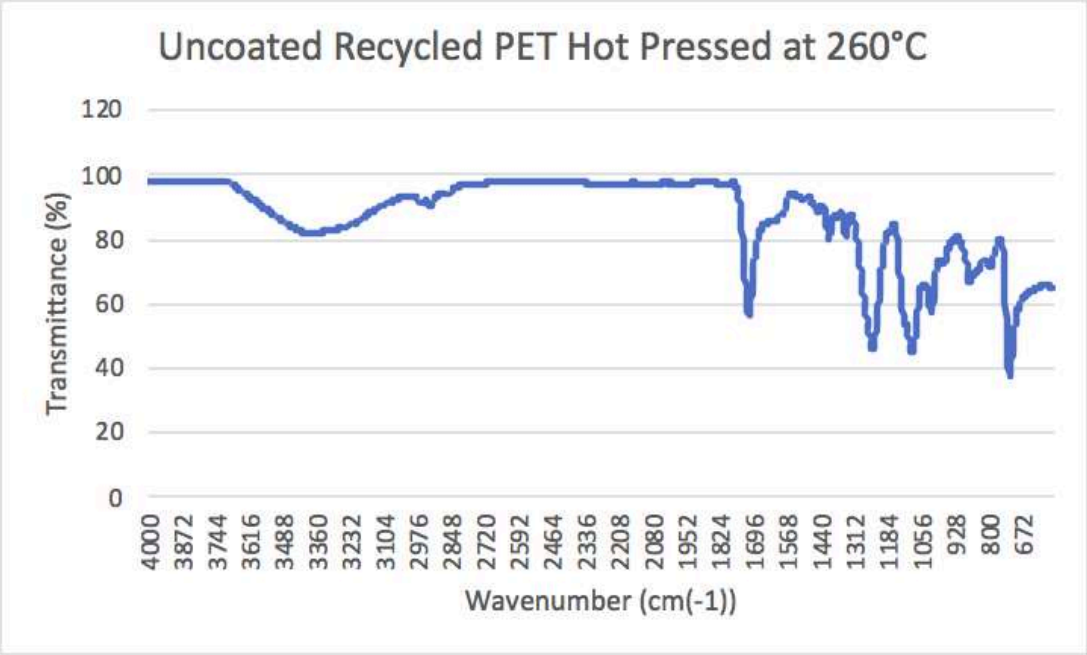

Figure 21: FTIR spectra of uncoated recycled PET hot pressed at 260°C

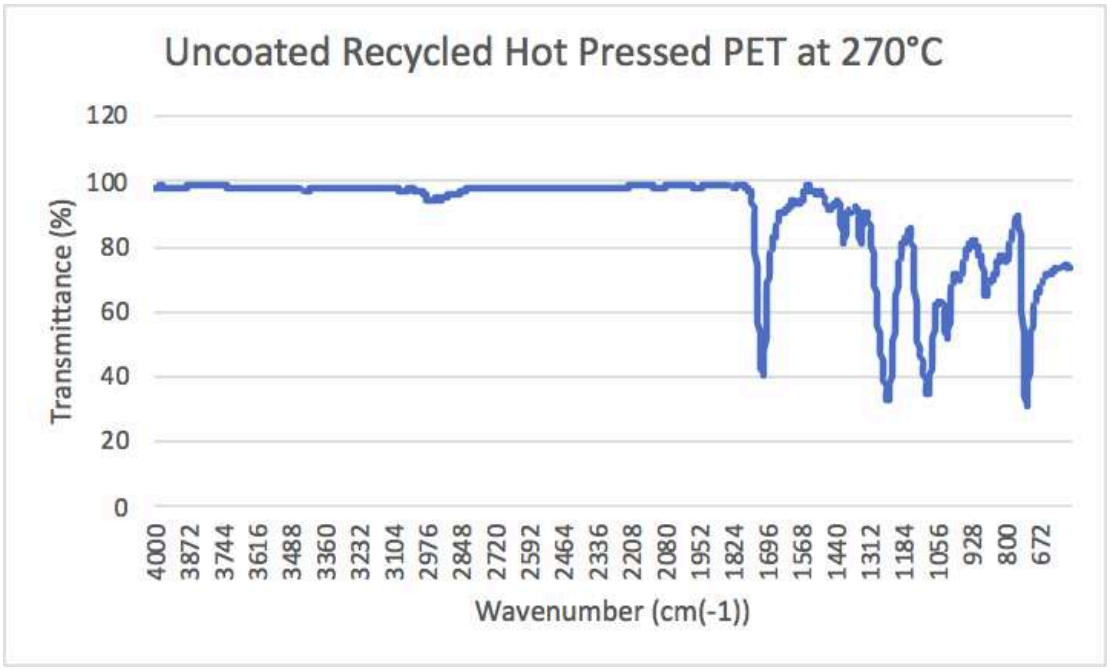

Figure 22: FTIR Spectra of uncoated recycled PET hot pressed at 270°C

Table 6: FTIR Spectrum Data Analysis of Uncoated PET Samples [17]

PET Sample Type	**FTIR Spectrum Values of Major Peaks**	**Within Spectrum Points Range**
Unrecycled PET	1710	✔
	1238	✔
	720	✔
	2926	✔
	3408	✔
Recycled PET	1710	✔
	1238	✔
	720	✔
	2916	✔
	3402	✔
Hot Pressed PET at 260°C	1714	✔
	1238	✔
	718	✔
	2920	✔
	3338	✔
Hot Pressed PET at 270°C	1712	✔
	1240	✔
	720	✔
	2916	✔
	3336	✔

Appendix B: FTIR Graphs of Coated PET and Data Points of Major Peaks

This appendix shows the FTIR spectra of coated PET within Figures 23 to 27 and highlights major peak data points within Table 7.

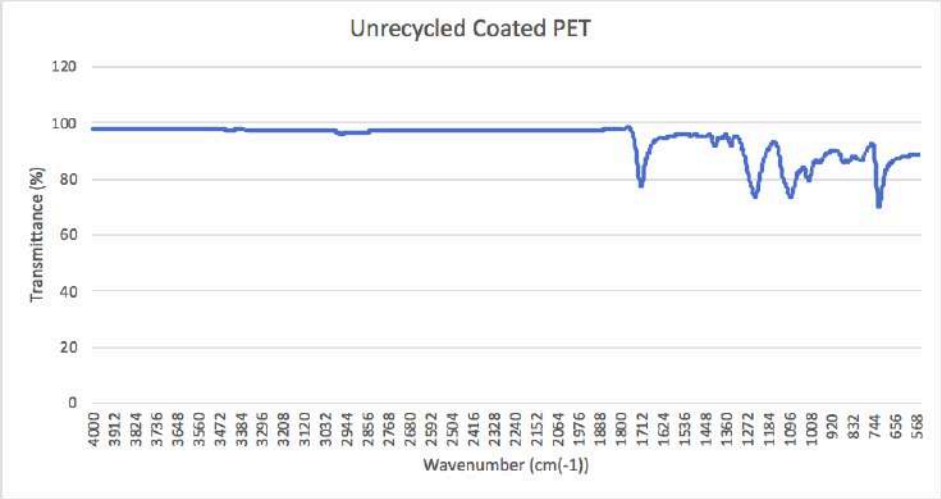

Figure 23: FTIR Spectra of coated PET

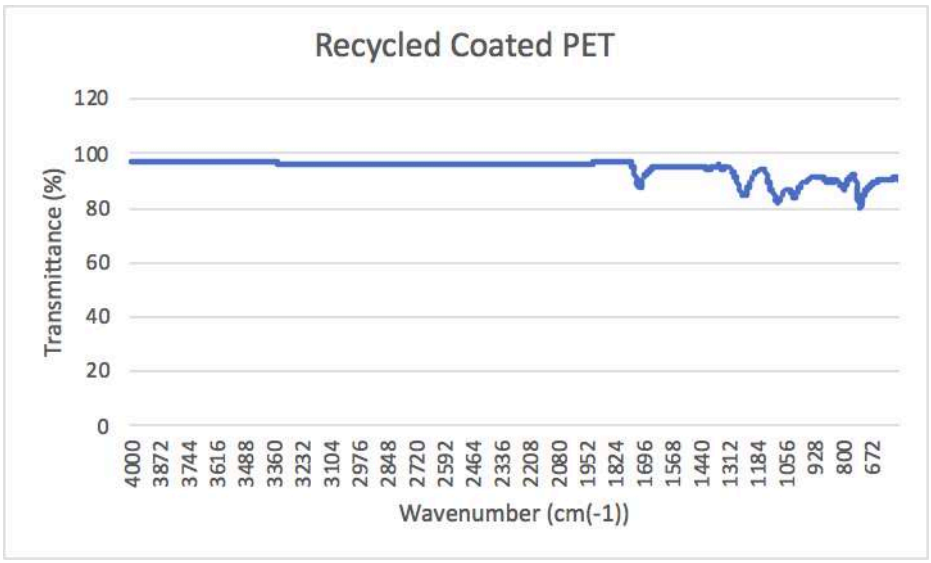

Figure 24: FTIR spectra of coated recycled PET

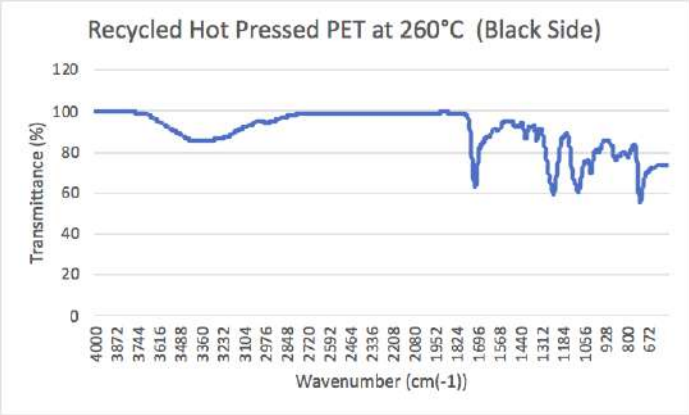

Figure 25: FTIR spectra of coated recycled PET hot pressed at 260°C for the black side

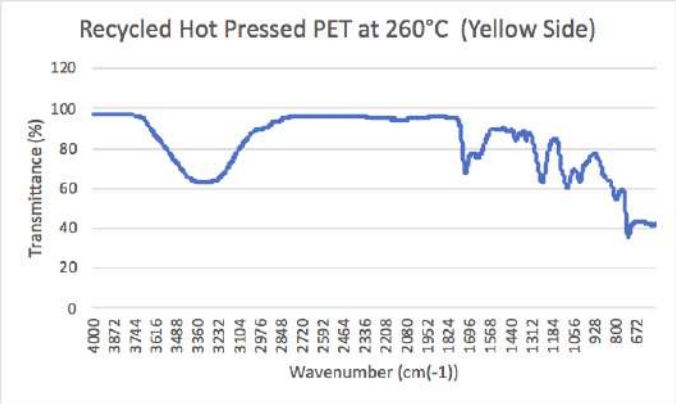

Figure 26: FTIR spectra of coated recycled PET hot pressed at 260°C for the yellow side

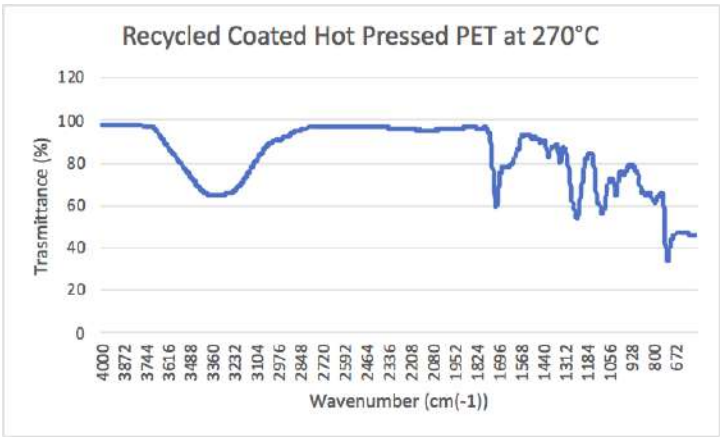

Figure 27: FTIR spectra of coated recycled PET hot pressed at 270°C

Table 7: FTIR Spectrum Data Analysis of coated PET Samples [17]

PET Sample Type	**FTIR Values of Major Peaks**	**Maintained PET Structure**
Unrecycled PET	1712	✔
	1238	✔
	718	✔
	2932	✔
	3392	✔
Recycled PET	1712	✔
	1238	✔
	718	✔
	2800	✔
	3330	✔
Hot Pressed PET at 260°C (Black Side)	1714	✔
	1240	✔
	720	✔
	2942	✔
	3396	✔
Hot Pressed PET at 260°C (Yellow FIbrous Side Side)	1714	✔
	1238	✔
	718	✔
	2922	✔

	3348	✔
Hot Pressed PET at 270°C	1710	✔
	1240	✔
	718	✔
	2898	✔
	3354	✔

Appendix C: Calculating Linear Regression Model for Tensile Tests

PET# is the labelling for uncoated samples and PETT# is the labelling for coated samples within the code block below. This code calculates the linear regression of the stress-strain graphs and outputs Young's modulus. The graphs of each individual sample is shown in Figures 28 to 37 below.

```
import os
import pandas as pd
import matplotlib.pyplot as plt
from sklearn.linear_model import LinearRegression

# Sample geometry
WIDTH = 15  # mm
THICKNESS = 5  # mm
GAUGE_LENGTH = 25  # mm

# File paths (update these if running locally)
file_paths = {
    "PET1": "/mnt/data/PET1.txt",
    "PET2": "/mnt/data/PET2.txt",
    "PET3": "/mnt/data/PET3.txt",
    "PET4": "/mnt/data/PET4.txt",
    "PET5": "/mnt/data/PET5.txt",
    "PETT1": "/mnt/data/PETT1.txt",
    "PETT2": "/mnt/data/PETT2.txt",
    "PETT3": "/mnt/data/PETT3.txt",
    "PETT4": "/mnt/data/PETT4.txt",
    "PETT5": "/mnt/data/PETT5.txt",
}

# Function to extract displacement and load data
def extract_data(file_path):
    with open(file_path, "r") as f:
        lines = f.readlines()

    # Locate where the numerical data starts
    start_idx = 0
    for i, line in enumerate(lines):
        if line.strip().startswith("1"):
            start_idx = i
            break
```

```
    data = []
    for line in lines[start_idx:]:
        parts = line.strip().split()
        if len(parts) == 3:
            try:
                displacement, load = float(parts[1]), float(parts[2])
                data.append((displacement, load))
            except ValueError:
                continue

    return pd.DataFrame(data, columns=["Displacement", "Load"])

# Function to calculate modulus and generate plot
def calculate_and_plot(sample_name, df, strain_limit=0.03):
    # Engineering stress and strain calculations
    df["Stress"] = (df["Load"] * 1000) / (WIDTH * THICKNESS)  # Convert kN to MPa
    df["Strain"] = (df["Displacement"] - df["Displacement"].iloc[0]) / GAUGE_LENGTH

    # Filter the linear region and remove slack (negative or zero stress/strain)
    linear_df = df[(df["Strain"] > 0) & (df["Stress"] > 0) & (df["Strain"] <=
strain_limit)].head(30)

    # Linear regression
    model = LinearRegression()
    model.fit(linear_df[["Strain"]], linear_df["Stress"])
    slope = model.coef_[0]  # This is Young's Modulus in MPa

    # Predict stress for linear fit line
    predicted_stress = model.predict(linear_df[["Strain"]])

    # Plot the full stress-strain curve and the linear fit
    plt.figure(figsize=(8, 5))
    plt.plot(df["Strain"], df["Stress"], label="Stress-Strain Curve")
    plt.plot(linear_df["Strain"], predicted_stress, '--', label=f"Linear Fit: {slope:.2f}
MPa")
    plt.title(f"{sample_name}: Stress-Strain with Linear Fit")
    plt.xlabel("Strain")
    plt.ylabel("Stress (MPa)")
    plt.legend()
    plt.grid(True)
    plt.tight_layout()
    plot_path = f"/mnt/data/{sample_name}_modulus_plot.png"
    plt.savefig(plot_path)
    plt.close()

    return slope / 1000, plot_path  # Return GPa and path to plot

# Main processing
results = []
plot_paths = []
```

```
for sample, path in file_paths.items():
    if os.path.exists(path):
        df = extract_data(path)
        modulus, plot_path = calculate_and_plot(sample, df)
        results.append((sample, modulus))
        plot_paths.append(plot_path)
    else:
        print(f"File not found: {path}")
        results.append((sample, None))
```

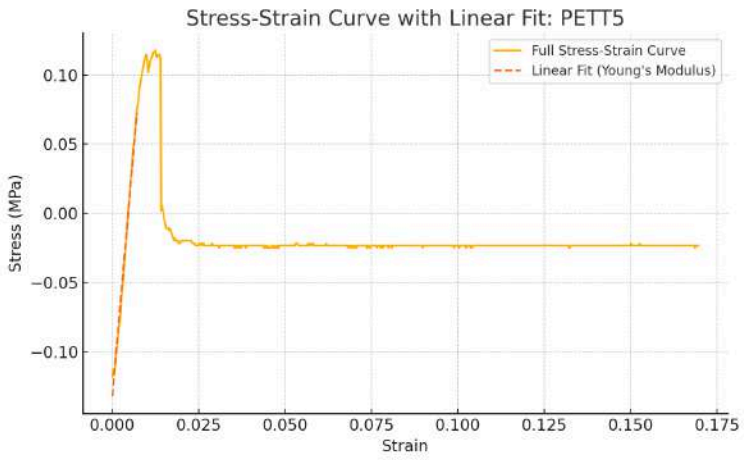

Figure 28: Stress-strain curve for coated sample #5

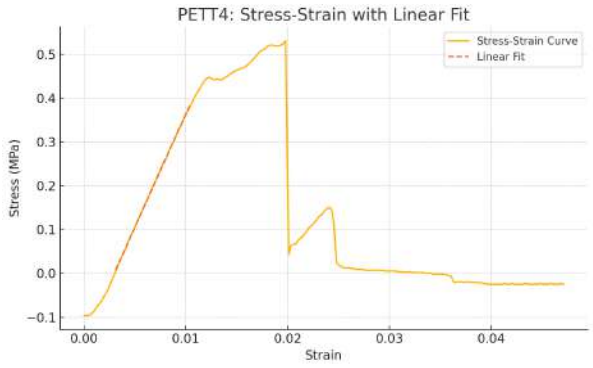

Figure 29: Stress-strain curve for coated sample #4

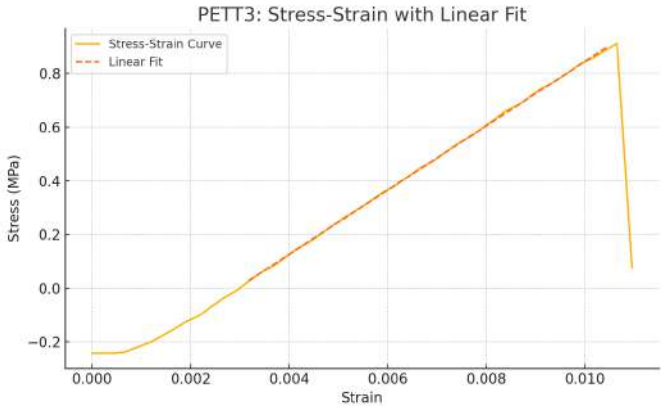

Figure 30: Stress-strain curve for coated sample #3

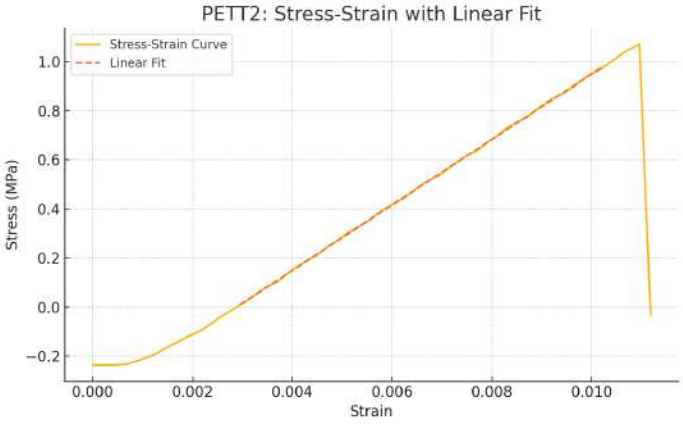

Figure 31: Stress-strain curve for coated sample #2

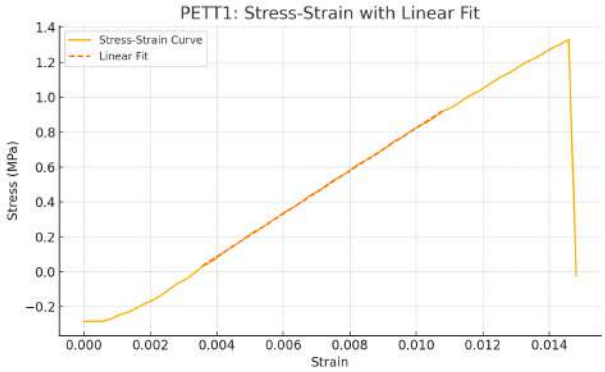

Figure 32: Stress-strain curve for coated sample #1

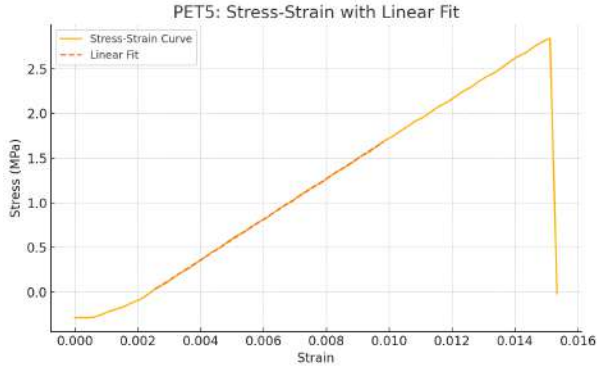

Figure 33: Stress-strain curve for uncoated sample #5

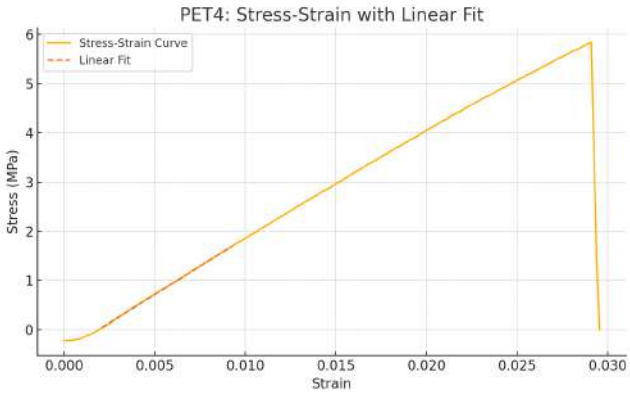

Figure 34: Stress-strain curve for uncoated sample #4

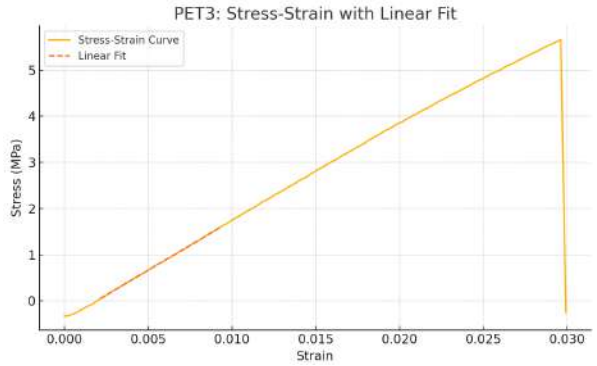

Figure 35: Stress-strain curve for uncoated sample #3

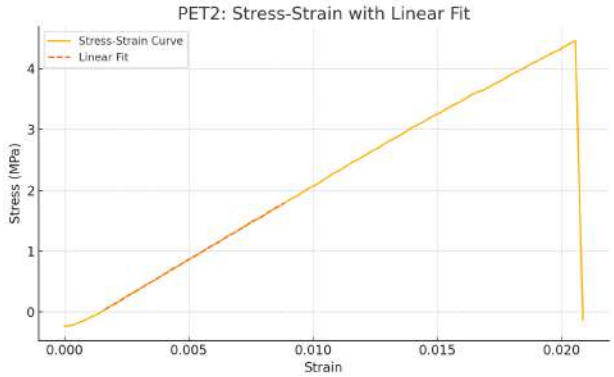

Figure 36: Stress-strain curve for uncoated sample #2

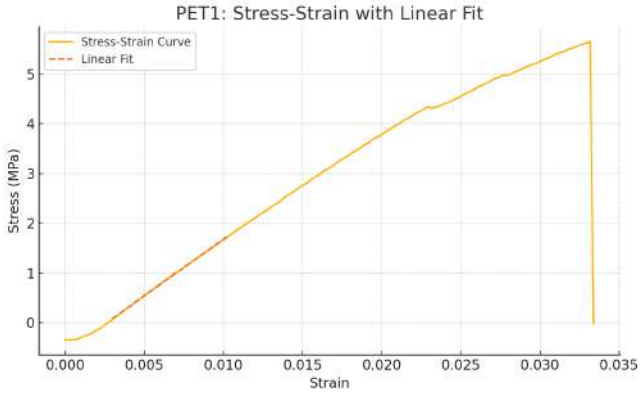

Figure 37: Stress-strain curve for uncoated sample #1

Appendix D: Stress-Strain Graphs for Coated and Uncoated PET Samples

This appendix describes the stress-strain curves for coated and uncoated samples within Figure 38 and 39.

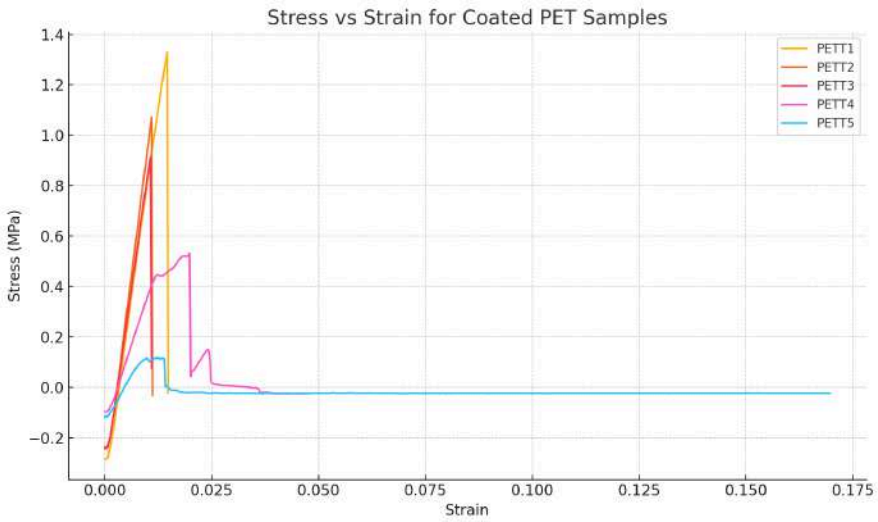

Figure 38: Stress-strain curve for coated PET

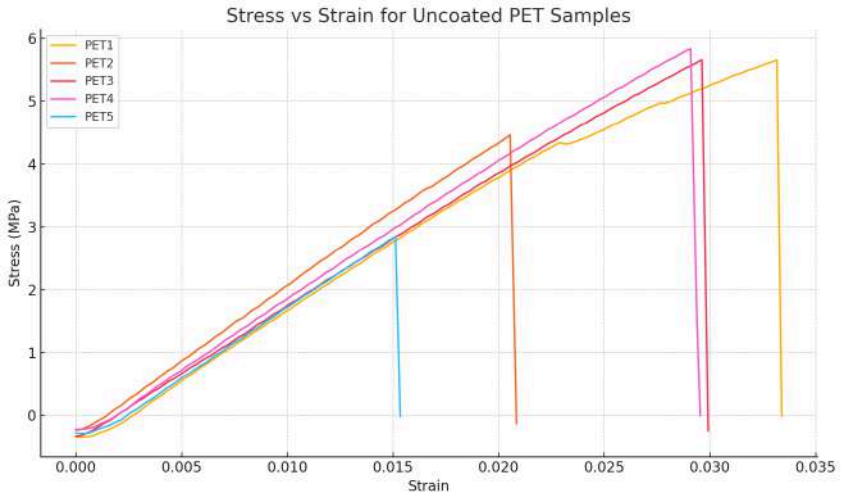

Figure 39: Stress-strain curve for uncoated PET